Molecular Mechanism of Gleditsiae Spina for the Treatment of High-grade Serous Ovarian Cancer Based on Network Pharmacology and Experimental Verification

Boran Zhang
Beijing University of Chinese Medicine
Wenchao Dan
Beijing University of Chinese Medicine
Xing Chen
Beijing Hospital of Traditional Chinese Medicine
Cunfang Dai
Beijing Hospital of Traditional Chinese Medicine
Guangda Li
Beijing University of Chinese Medicine
Tingting Ma
Beijing Hospital of Traditional Chinese Medicine
Xinjie Chen
Beijing Hospital of Traditional Chinese Medicine
Xiaohui Yin
Beijing University of Chinese Medicine
Ganlin Zhang
Beijing University of Chinese Medicine
Xiaomin Wang (wangxiaomin_bhtcm@126.com)
Beijing Hospital of Traditional Chinese Medicine https://orcid.org/0000-0003-1274-224X

Research

Keywords: active ingredients, Gleditsiae Spina, high-grade serous ovarian cancer, network pharmacology

Posted Date: August 11th, 2021

DOI: https://doi.org/10.21203/rs.3.rs-744923/v1

Abstract

Background

In this study, we aimed to analyze the pharmacological mechanism of Gleditsiae Spina in the treatment of high-grade serous ovarian cancer (HGSC) based on network pharmacology and *in vitro* experiments.

Methods

The main active ingredients of Gleditsiae Spina were identified by high performance liquid chromatography and mass spectrometry, and ADME screening was performed. The component targets of Gleditsiae Spina were screened using the pharmMapper platform, and differentially expressed genes in normal and HGSC tissues were identified through GEO database. Thereafter, Cytoscape 3.7.2 software was used to construct the network of "active ingredient-targets," and the BioGenet database was used for protein-protein interaction analysis. Furthermore, the protein-protein interaction network was established, and the potential protein function module was mined. Biological processes and pathways were analyzed through gene ontology and Kyoto Encyclopedia of Genes and Genomes analysis.

Results

The core active ingredients of Gleditsiae Spina for regulating HGSC included luteolin, genistein, D-(+)-tryptophan, ursolic acid, and berberine. The ideal targets were *HPSE, PI3KCA*, *AKT1*, and *CTNNB1*. The prediction results were verified by molecular docking, molecular dynamics simulation, and western blot analysis.

Conclusions

This study revealed the mechanism of Gleditsiae Spina for the treatment of HGSC based on multi-components, multi-targets, and multi-channels. It also provides a theoretical basis for the prevention of ovarian cancer and its treatment using traditional Chinese medicine in the future.

Background

As one of the most serious diseases in women, ovarian cancer causes 152 000 deaths per year worldwide, ranking fourth among female tumour deaths (1-3). The majority of patients are diagnosed at the advanced stage of ovarian cancer due to the lack of obvious symptoms, and reliable diagnostic tools (4). Therefore, improving ovarian cancer treatment, particularly highly serous ovarian cancer (HGSC), has great clinical significance. As an aggressive cancer, HGSC often shows aneuploidy and mutations and is considered to be highly malignant, and their clinical prognosis is worse than other classifications (5). Operative treatment includes total abdominal hysterectomy, bilateral salpingo-oophorectomy, removal of

pelvic and para-aortic lymph nodes and omentum, and other complementary procedures (such as appendectomy), combined with the usage of platinum drugs and taxane-like chemotherapy (6). Traditional treatments including cytoreductive surgery and platinum-based chemotherapy, may cause 75-80% of relapses (7). Some patients will experience recurrence and resistance to chemotherapy after undergoing conventional treatment, and the overall survival of HGSC patients has not been noteworthy in the past 30 years.

Currently, traditional Chinese medicine (TCM) is being increasingly recognized due to its effectiveness in alleviating illnesses with minimal side effects (8). The application of TCM in the treatment of tumours is also increasing extensively in China, and most Asian countries. It plays an important role in the prevention and treatment of precancerous lesions, postoperative recurrence of tumours, reduction of toxic side effects of western medicine, and maintenance of advanced tumours (9). In a previous meta-analysis, the combination of TCM treatments and western medicine significantly improved the KPS score, CA125 level, and 3-year survival rate in the postoperative adjuvant treatment of ovarian cancer (10). The Chinese herbal medicine “Shenlinglan Capsule” can attenuate ovarian cancer migration by inhibiting the expression of glycogen synthase kinase 3 (GSK-3) in vitro (11). Studies have shown that “Jianpi Huayu Decoction” can alleviate the progression of liver cancer. Jianpi Huayu Decoction can reduce the expression of reactive oxygen species (ROS) in myeloid-derived suppressor cells (MDSCs) by regulating its suppression in the immune system, attenuate inhibition of CD4 cell proliferation, and aid in the treatment of liver cancer (12). Bufalin in the TCM “Chan su” can regulate the cell cycle, inhibit receptor phosphorylation, and tumour cell proliferation (13). Gleditsiae Spina, a Chinese medicine with well-defined phytochemicals, has been proven a useful therapeutic agent in clinical treatment for ovarian cancer and effective in clinical applications. Gleditsiae Spina is often used as an alternative remedy in the treatment of ovarian cancer, which can improve symptoms such as lower abdominal discomfort. Biological activity of Gleditsiae Spina include detoxification, reduction of swelling and purulence, wound healing, bloated dystocia etc. (14). High-performance liquid chromatography elucidated various flavonoids present in Gleditsiae Spina extracts, which confers anti-inflammatory, antibacterial, and anti-tumour effects (15). Hence, it is widely used in clinical practice. Ethanol extracts of Gleditsiae Spina maintain tumour cells in G2/M phase, regulate phosphorylation of extracellular signal-regulated kinases (ERK), tumour necrosis factor-alpha (TNF-α), matrix metalloproteinase-9 (MMP-9) expression, and other processes to inhibit tumour cell growth (16). However, its molecular mechanism of action is yet to be elucidated. Therefore, studying the active ingredients, targets, and molecular pathways of Gleditsiae Spina can elucidate molecular mechanisms and expand its clinical applications.

With the development of network technology and bioinformatics, network pharmacology is gradually becoming a novel tool in elucidating molecular mechanisms and pharmacological effects (17). It can effectively establish a “compound-protein/gene-disease” network and reveal the mechanism of small molecules through high-throughput methods (18). Furthermore, networks can be constructed between various components to analyse their mutual relationships. Careful investigation of the key nodes in the network can systematically explain the material basis and mechanisms of Chinese medicines. Therefore, in this study, the Chinese medicine network pharmacology method was used to establish a starting point

of the differential genes of HGSC and normal patients, where gene targets of Gleditsiae Spina, and the predicted Protein-Protein Interaction (PPI) network were intersected. The data mining method was used to obtain the candidate genes that Gleditsiae Spina acts on in HGSC. PPI network diagrams, Gene ontology (GO) enrichment analysis, Kyoto Encyclopedia of Genes and Genomes (KEGG) signal pathways and gene-signal pathway network diagrams were used to systematically predict and explore the potential active ingredients and key therapeutic targets of Gleditsiae Spina interference in HGSC.

Materials And Methods

Mass Spectrometry Analysis of Gleditsiae Spina

Production of Freeze-dried Powder of the Gleditsiae Spina

Gleditsiae Spina, mainly used as medicine, is obtained from the dry spines of the leguminous *Gleditsia sinensis* Lam. In this study, Gleditsiae Spina was provided by Beijing Xinglin Pharmaceutical Co. (Beijing, China), and identified by Professor Mao Kechen according to the Chinese Pharmacopoeia standards.

Gleditsiae Spina pieces (200 g) were placed in a vessel and cooked twice for 1 h each time. The two resulting decoctions were mixed to obtained a volume of 450 mL which was transferred to a vacuum freeze dryer (Epsilon 2-4LSC; Martin Christ Gefriertrocknungsanlagen, Harz, Germany) to obtain 18.72 g of freeze-dried powder, with a production rate of 8.28%. The powder was placed into a closed container containing silica gel to keep it dry. The powder was dissolved in deionized water to prepare a 100 mg/mL solution and stored at −20 °C for subsequent experiments.

Identification of the Gleditsiae Spina Components Using High Performance Liquid Chromatography and Mass Spectrometry

Gleditsiae Spina freeze-dried powder (100 mg) was dissolved in 50% methanol and sonicated for 10 min. The solution was centrifuged at 3,000 r/min for 5 min (Beckman Coulter, Brea, CA, USA), the supernatant was collected and filtered through a 0.22 μm filter (Millipore, Burlington, MA, USA). The filtered solution was subjected to mass spectrometry analysis using a Q-Exactive Orbitrap quadrupole-electrostatic field orbitrap mass spectrometer equipped with a thermal spray ion source and a Vanquish ultra-high performance liquid chromatography system (Thermo Fisher Scientific, Waltham, MA, USA).

Target Prediction

Prediction of Active Components in Gleditsiae Spina

Based on the mass spectrometry results of Gleditsiae Spina, the active ingredients were initially selected. The molecular structure of the active pharmaceutical ingredients and 3Dsdf were obtained on the Pubchem platform. The 3Dsdf files of the active ingredients were uploaded to the SwissADME platform, and the pharmacokinetics and drug similarity were screened. The compound ingredients were required to have good gastrointestinal absorption, and the drug similarity received more than 3 positive evaluations.

The potential targets of the ingredients were predicted on the PharmMapper platform (19).We required the norm fit value to be greater than 0.75

Construction of the Active Ingredient-Target Network of the Gleditsiae Spina

The “active ingredient-target” network of the Gleditsiae Spina was constructed and analyzed by Cytoscape 3.7.2 software (20). "node" was used to indicate the component or target, and "edge" was used to indicate the relationship among them. The “Network Analyzer” analyzing tool built in Cytoscape 3.7.2 software was used to analyze the network characteristics, including Degree, Betweeness, and Closeness, to study important components and target relationships of Gleditsiae Spina.

Ovarian Cancer-Related Targets

The differentially expressed genes of patients with ovarian cancer were obtained from GEO database (Series: GSE54388 and GSE14407, Samples: normal tissue GSM1314222-GSM1314227,GSM360039-360049, GSM359984 and tumor tissue GSM1314228-GSM1314243, GSM359972-359983). Differential Genes with an adj. *P*-value < 0.05 and |log2(fold change)|>1 were considered to be of significantly differential expression and ovarian cancer-related targets.

Construction of protein interaction network and screening of key targets

The PPI were constructed by BisoGenet3.0 (21). The targets related to the active ingredients of Gleditsiae Spina, and the targets of disease were introduced into BisoGenet, each generated a PPI network. The intersection network of the two PPI networks was extracted through the Merge function in Cytoscape, and CytoNCA2.1 (22) was used to analyse the nodes of the intersection network. The targets were mapped and visualized by Cytoscape 3.7.2 and the protein-protein internetwork (PPI) of the shared genes were constructed through the String APP in Cytoscape.

Pathway enrichment analysis

The Metascape platform (23) was used to perform pathway enrichment analysis on the target. The platform integrates many authoritative functional databases such as GO, KEGG, etc., and supports batch genes or annotates, enriches and analyses proteins and builds PPI networks. The platform is updated once a month to ensure data is reliable. Imported potential ovarian cancer targets were inserted into the Cytoscape platform for GO and KEGG analysis, the results were saved and visualized with R software3.6.1.

Molecular Docking and Molecular Dynamics Simulation

In order to further determine the credibility of the relationship between the ovarian cancer target and the core components of Gleditsiae Spina, the top two compounds of traditional Chinese medicine-compound-target were selected as ligands genistein and luteolin, and four important targets were selected to analyse molecularly docking.

First, the crystal structure of the three proteins in pdb format from the RCSB database was downloaded, and the SDF from the PubChem database. We also downloaded the 3D chemical structure of the candidate compound and used Open Babel 2.4 to convert to the pdb format file. AutoDock Tools 1.5.6 was used to delete the water molecules in the ligand, separate the ligand from the receptor, add non-polar hydrogen, calculate the Gasteiger charge, and save the pdbqt format file. The selected potential core constituent ligands were subjected to energy minimization treatment, the ligand atom type was given, the charge was calculated, and stored in pdbqt format. Molecular docking operations were performed using Autodock Vina 1.1.2, and reflect the matching degree and docking activity between the target and the ligand through the docking score value, where we believe that a docking score > 4.25 means that the ligand and the target have binding activity, a score > 5.0 means good matching activity, and a score > 7.0 means strong docking activity (24).

The MD simulation of docked complexes were carried out using Desmond version 2020. Here, OPLS3e force field was used to initiate the MD simulation, and the system was solvated using TIP3 water model. The neutralization of the system was performed by adding counter ions. Energy minimization of the entire system was performed using OPLS3e, as it is an all-atom type force field. The geometry of water molecules, the bond lengths and the bond angles of heavy atoms was restrained using the SHAKE algorithm. Simulation of the continuous system was executed by applying periodic boundary conditions and long-range electrostatics was maintained by the particle mesh Ewald method. The equilibration of the system was done using NPT ensemble with temperature at 300 k and pressure at 1.0 bar. The coupling of temperature-pressure parameters was done using the Berendsen coupling algorithm. On post-preparation of the system, the production run was performed for 200 ns with a time step of 1.2 fs and trajectory recording was done for every 200 ps summing up to the recording of 10,00 frames. The calculation of the RMSD (Root mean square deviation) was done for the backbone atoms and was analyzed graphically to understand the nature of protein-ligand interactions. RMSF (Root Mean Square Fluctuation) for every residue was calculated to understand the major conformational changes in the residues in comparison between the initial state and dynamics state.

Cell Verification

Cells and cell proliferation

Human ovarian cancer cell line A2780 purchased from ATCC was used in this study. A2780 cells were cultured in RPMI-1640 (Gibco Company, USA) with 10% foetal bovine serum (Gibco Company, USA) and 1% penicillin-streptomycin (Gibco; 10000 units/mL Penicillin, 10000 μg/mL Streptomycin) and cultured at 37°C in a humidified atmosphere under 5% CO2. Cells used in this experiment were in the exponential growth phase.

For proliferation tests, The MTT was used to evaluate cell proliferation.3000 cells were seeded in each of the non-edge well of 96-well plates. Freeze-dried powder of the Gleditsiae Spina was added after the cells adhered to the wall. The freeze-dried powder of maximum freezing 20 mg/mL degree was diluted into the cells by multiple dilutions. After 24 hours, 20 μL of 3-(4,5-dimethylthiazol-2-yl)-2,5-diphenyltetrazolium

bromide (MTT) (Sigma, St. Louis, MO, USA) solution (5 mg/mL in phosphate-buffered saline (PBS)) was added to the culture medium in each well at a final concentration of 0.5 mg/mL and the cells were incubated at 37 °C for 4 hours. The supernatants were replaced with 150 μL of dimethyl sulfoxide (Sigma, St. Louis, MO, USA). Then the 96-well plates were measured by Microplate reader at 490 nm.

Western blot

After exposure to the test compounds (1.25mg/mL, 2.5 mg/mL Freeze-dried powder of the Gleditsiae Spina) for 24 h, the A2780 cells were harvested and lysed with RIPA lysis buffer (Beyotime Biotechnology, Beijing, China) containing Protease Inhibitor Cocktail Set III (Calbiochem, San Diego, CA, USA). A2780 cell lysates were centrifuged at 12,000 rpm for 15 min at 4 °C, and the supernatants were collected. The protein concentration was determined using the Pierce BCA Assay Kit (Thermo Scientific, Rockford, IL, USA). Equal amounts (30 μg/lane) of total protein were separated by 10% SDS-PAGE and transferred onto PVDF membranes. The membranes were blocked with 5% BSA (Amresco, Solon, OH, USA) at room temperature for 1 h and incubated overnight at 4 °C with the following primary antibodies: anti-HPSE1(1:1000, CST,USA), anti-MMP9(1:1000, CST,USA), anti-β-Catenin(1:1000, CST, USA), anti-N-cad (1:1000 CST, USA), anti-E-cad(1:1000 CST, USA),anti-PI3K/p-PI3K (1:1000, CST,USA), anti-AKT/p-AKT (1:1000, CST,USA), anti- YAP/TAZ(1:1000, CST,USA)and β-actin (1:10000, CST,USA). After washing the membranes in Tris-buffered saline with 0.1% Tween-20 (TBST), the membranes were probed with secondary antibodies (1:10,000) for 1 h at room temperature. The signals were detected using an Odyssey Infrared Imaging System (Li-cor Biosciences, Lincoln, NE, USA). The relative density of the protein bands was measured by Odyssey version 3.0 software (LI-COR Biosciences). Each experiments were repeated three times. The ratios of the protein band intensities relative to that of β-Actin were calculated for each sample using Image J.

Results

Mass spectrometry results

The extract of Gleditsiae Spina was analyzed according to the method in 2.1, and the total ion current diagram under the positive and negative ion mode was obtained (Figure 1). According to the retention time of each chemical component, high-resolution precise molecular weight, MSn multi-level fragment information obtained by LC-MS detection, combined with the extracted ion current map and standard product information, Mzcloud database and related literature, the composition was confirmed, and a total of 39 were identified. (See Table 1 for the results). Among them, the number identified in the positive ion mode is 30, the number identified in the negative ion mode is 18, and the 9 compounds are the compounds identified by the positive and negative ions.

Network Construction and Target Prediction

Active Ingredients and Targets of Gleditsiae Spina

Thirtynine Gleditsiae Spina components were observed in 3.1, screened according to the pharmacokinetics and drug similarity in SwissADME platform, and supplemented according to previous literature reports. This resulted in 26 active components. The SDF structure of 26 selected components were obtained from Pubchem, and the PharmMapper target prediction model was used to predict the above 26 targets of active ingredients. The 26 medicinal active ingredients are shown by in Table 2. Relevant target prediction technology was used to predict the active targets, eliminating duplicate targets, and a total of 610 predicted targets were obtained, as shown in Figure 2.

Construction and Analysis of "Active Ingredient-Target" Network

Cytoscape 3.7.2 was used to draw and analyse the relationship network between the effective components of Gleditsiae Spina and its active targets, a total of 635 nodes (including 609 targets and 26 active components) and 1090 relationships were obtained. The size represented the corresponding Degree value. The larger the node area was, the larger the Degree value, indicating that the more biological functions involved, the higher its biological importance (Figure 2).

Ovarian Cancer-Related Target Searching

Ovarian cancer-related targets (1483) were identified from the Gene Expression Omnibus (GEO) database. Figure 3 shows heat maps and volcano maps indicating the distribution of differentially expressed genes, which are represented by red dots on the map.

Screening of Key Targets for Gleditsiae Spina Treatment in Ovarian Cancer

To obtain richer node-node connection information in PPI networks, the efficiency of node information transmission was optimized, the targets that play an important role in the network were identified, and the network topology characteristic attributed values of the above-mentioned intersection PPI network graph was calculated. Through two screenings, a total of 87 key targets were obtained. The targets were shown in Figure 4-A and the PPI network of the key genes was shown in Figure 4-B.

Pathway Enrichment Analysis and Visualization of Gleditsiae Spina Treatment for Ovarian Cancer

Metascape platform was used to perform gene enrichment analysis on the above 87 key nodes, including GO-BP (Biological Process), GO-CC (Cellular Component), GO-MF (Molecular Function) and KEGG pathway. R (version 6.1) was used to draw KEGG pathway a bubble chart (shown in Figure 5). The bubble colour changed from red to purple to indicate that the log *P* value is from small to large. The smaller the log10(*P*) value, the stronger the significance, and the larger the bubble, the larger the gene count (Count value) of the pathway.

Molecular docking and Molecular Dynamics Simulation results

The three core potential compounds luteolin and genistein were molecularly docked with the four core targets PIK3CA, CTNNB1, HPSE and AKT1 to obtain the group receptor-ligand docking results. Among the

nine groups, the highest docking score is for luteolin-HPSE (-8.97 kcal/mol), and the lowest docking score is for genistein- HPSE (-7.35 kcal/mol). This indicates that the selected potential core compounds have better binding activity with the target. The diagram depicting eight docking modes is shown in Figure 6. It can be seen from the figure that each ligand is embedded in the active pocket of the target and that it interacts with multiple residues of the target through hydrophobic interactions and hydrogen bond formation.

Next Genistein, Luteolin, and Berberine as the core components in the network were selected to perform molecular dynamics simulation tests with AKT1, HPSE, and PI3K. The binding of Genistein and Luteolin to the ligand quickly stabilized and continued to work and after a short period of fluctuation, the binding of Berberine to the ligand also forms a stable state. The results were shown in Figure 7.

Verification of Therapeutic Effects of Gleditsiae Spina in Ovarian Cancer

Next, we conducted *in vitro* experiments to verify the therapeutic potential of Gleditsiae Spina. The MTT assay was performed to evaluate the viability of A2780 cancer cells treated with increasing concentrations of Gleditsiae Spina solution (156.25–20,000 μg/mL) for 24 and 48 h. The cell viability decreased with the increase of the Gleditsiae Spina concentration. To further explore the therapeutic mechanisms of Gleditsiae Spina in combination with the above-described KEGG analysis data, HGSC cells were stimulated with 1.25 and 2.5 mg/mL Gleditsiae Spina solution for 24 h, followed by protein extraction and analysis by western blotting, with heparinase used as Core (Figure 8B–D). Our results showed that the levels of heparinase 1, MMP9, β-catenin, and N-cadherin were significantly downregulated in ovarian cancer cells in response to Gleditsiae Spina treatment in a dose-dependent manner. However, the level of E-cadherin increased in the high-dose group, although the increase was not statistically significant. Furthermore, treatment with Gleditsiae Spina inhibited the expression of proteins associated with the PI3K/AKT/mTOR pathway; however, expression of these molecules increased at higher doses of Gleditsiae Spina. This may be attributed to the interaction between the complex components of traditional Chinese medicine and the cells, which lead to programmed cell death. At high Gleditsiae Spina concentrations, only a small number of cells survived for more than 48 h. Therefore, although the autocompensation mechanism of cells can be ruled out, the specific mechanism in vivo needs to be further explored.

Discussion

Traditional Chinese medicine has a long history and has nurtured the Chinese nation for millennia. It protects human health through dialectical theory. Traditional Chinese medicine works against diseases through a single or compound prescription by multiple ingredients and targets. The cause of ovarian cancer is considered to be the accumulation of pathological products in TCM theory, and Gleditsiae Spina has the potential to clear these toxic metabolites. It is a summary of experience obtained in clinical practice of TCM and has obvious clinical effects based on clinical experience. The concept of network

pharmacology and the theory of TCM have similar aspects, which can explore the unknown mechanism of action of Chinese herbal medicine from the perspective of overall composition and function(25).

Based on the mass spectrometry results, along with previously reported data, we inferred that luteolin, genistein, D-(+)-tryptophan, ursolic acid, and berberine in the Gleditsiae Spina play a core role in the treatment of ovarian cancer. It was previously reported that D-(+)-tryptophan exhibits anticancer activity, which can stimulate mTORC1 and enhance the activity of T-cells within the tumor microenvironment (26). Luteolin is a flavonoid compound that inhibits tumor cell proliferation, blocks cell cycle, and reverses tumor epithelial-mesenchymal transition (27). Luteolin downregulates the expression of aromatase, and consequently inhibits estrogen synthesis in ovarian cancer (28). Genistein can modulate the cell cycle and regulate the ERK1/2, NF-κB, Wnt, β-catenin, and PI3K/Akt signaling pathways to exert its anticancer effects. Moreover, it can synergize with paclitaxel and other ovarian cancer drugs (29). Ursolic acid can downregulate the expression of YAP1 of the hippo pathway in tumor treatment (30). Studies have shown that berberine can induce apoptosis in various tumor cell lines. By inhibiting the transcriptional activity of β-catenin, berberine modulates the Wnt signaling pathway (31), and increase the expression of caspase-3 and -8; thus, it promotes apoptosis of ovarian cancer cells, when used in combination with cisplatin (32).

The KEGG results showed that Gleditsiae Spina affects ovarian cancer development via multiple pathways and thus plays a therapeutic role. The expression levels of heparinase 1, MMP9, β-catenin, N-cadherin, PI3K/AKT/mTOR, as well as their phosphorylation levels, which are involved in tumor progression, were reduced after treatment with Gleditsiae Spina.

Proteoglycans are widely distributed on the cell surface and in the cytoplasmic matrix; moreover, they play an important role in tumor development. Their glycosaminoglycan chains are modulated by heparinase, the only endoglycosidase in mammals; hence, heparinase plays an important role in regulating the function of proteoglycans (33). Several studies have found that the expression of heparinase is positively correlated with malignancy, with heparinase overexpressing tumors being associated with a worse prognosis compared with tumors in which heparinase is underexpressed (34).The extracellular matrix is mainly composed of keratansulfate proteoglycans, chondroitin sulfate proteoglycans, and dermatan sulfate proteoglycans (35); therefore, heparinase can accelerate the remodeling of tumor extracellular matrix and basement membrane (36) and contribute to tumor. Moreover, the cleaved heparan sulfate proteoglycans can bind to growth factors and increase the expression of VEGF by promoting p38 phosphorylation and Src kinase activity (37), thereby promoting angiogenesis and accelerating tumor metastasis and invasion (38). Our *in vitro* experiments showed that Gleditsiae Spina can inhibit the tumor growth and downregulate heparinase expression in tumor cells. By reducing the expression of heparinase, Gleditsiae Spina can regulate signaling cascades within the tumors (39).

MMP9 plays an important role in tumor extracellular matrix remodeling and communication between tumor cells (40). MMP9 is considered a potential biomarker for tumors, including ovarian cancer (41). Our western blotting results showed that Gleditsiae Spina significantly inhibits the expression of MMP9 to

reduce tumor cell activity. E-cadherin is a calcium ion-dependent transmembrane protein closely related to cell adhesion. Adjacent cells interact via an extracellular domain of E-cadherin, which is connected to β-catenin and the cell cytoskeleton. Thus, E-cadherin expression is negatively correlated with the degree of tumor invasion (42). Numerous studies have shown that the conversion of E-cadherin to N-cadherin often indicates the completion of the epithelial–mesenchymal transition process. Herein, although the expression of E-cadherin was low and changes in its expression could not be measured, the expression of N-cadherin was inhibited after treatment with Gleditsiae Spina, indicating that Gleditsiae Spina can reverse the expression of the two proteins, thereby inhibiting tumor development. β-catenin is a cytoplasmic protein, and its nuclear expression plays a role in activating transcription factors. Abnormal expression of β-catenin is related to the hippo and HIF1 signaling pathways, and it can also activate the Wnt signaling pathway (43). Moreover, its abnormal expression is closely related to colon cancer (44) and cervical cancer. Our western blotting results showed that Gleditsiae Spina inhibited the expression of β-catenin protein, which were consistent with the prediction results of the network pharmacology.

The PI3K/AKT/mTOR signaling pathway plays key role in cancer, as is related to cell proliferation, angiogenesis, chemotherapy resistance, and several other pathological conditions. Its downstream molecule mTOR can accelerate the formation of tumor stem cells (45), leading to tumor progression and relapse. Overexpression of PI3K can lead to *RAS* mutations, loss of *PTEN*, and is associated with HIF1, hippo, and MAPK signaling pathways. Moreover, it activates the epidermal growth factor receptor, stimulates the expression of the vascular endothelial growth factor, and accelerates angiogenesis (46). Approximately 70% of ovarian cancer patients present with overexpressed PI3K/AKT/mTOR cascade (47); thus, using inhibitors to target this pathway is an important strategy to treat ovarian cancer. In our study, Gleditsiae Spina significantly inhibited the expression of PI3K and AKT; low-dose treatment with Gleditsiae Spina inhibited the phosphorylation of AKT and mTOR, whereas the remarkably increased phosphorylation in the high-dose-treated group suggested its own S6K1-IRS1 negative feedback. Additional experiments are warranted to elucidate the underlying mechanism of the regulatory effect exerted by Gleditsiae Spina.

The molecular docking experiments can predict the binding ability of the ligand and the target at the molecular level. Using this approach, we determined that several components of Gleditsiae Spina have high binding ability to the ovarian cancer targets. Gleditsiae Spina can interfere with the activities of heparinase 1, β-catenin, PI3K, and AKT at the molecular level, thereby proving that Gleditsiae Spina can exert significant therapeutic effects on ovarian cancer. Molecular dynamics simulations, which can monitor time-resolved motions of molecules (48), further showed that the ingredients of Gleditsiae Spina stably interact with the disease-specific molecules in ovarian cancer, which indirectly provides a basis for verifying its therapeutic efficacy.

Cancer is a complex systemic disease characterized by complex, mutual feedback mechanisms of multiple pathways. This explains why many patients fail to respond to treatments targeting a single molecule. Traditional Chinese medicine is also a complex system. The interaction of complex components of traditional Chinese medicine, as well as the interactions between traditional Chinese

medicine components and the human body may be useful in treating diseases including cancers. Nevertheless, these interactions and their target mechanisms remain to be elucidated in vivo.

Conclusions

In this study, we adopted a network pharmacology approach to explore the mechanisms underlying the therapeutic effects of Gleditsiae Spina on HGSC. Our data demonstrates that Gleditsiae Spina can modulate the cytoplasmic matrix components and structure. Moreover, luteolin, genistein, D-(+)-tryptophan, ursolic acid, and berberine were identified among its main pharmacological components. Overall, Gleditsiae Spina was found to modulate various biological processes and pathways, including cell cycle, apoptosis, ubiquitin-dependent protein metabolism, viral infection and carcinogenesis, chromatin, transcription factor binding protein structure, and binding ability. Herein, *HPSE, PI3KCA, AKT1*, and *CTNNB1* were identified as the key target genes involved in therapeutic outcomes of ovarian cancer, which needs further exploration and validation in future studies. Our study outcomes provide new insights for designing new experimental models and strategies to validate the therapeutic targets in ovarian cancer proposed in this study. Furthermore, detailed analysis of the molecular mechanism involved in Gleditsiae Spina-mediated therapeutic effects on ovarian is warranted.

Abbreviations

ADME, absorption, distribution, metabolism and excretion; HGSC, high-grade serous ovarian cancer.

Declarations

Ethics approval and consent to participate: Not applicable.

Consent for publication: Not applicable.

Availability of data and materials: The datasets GSE54388 and GSE14407 for this study can be found in the Identification of differentially expressed transcription factors in ovarian cancer (https://www.ncbi.nlm.nih.gov/geo/query/acc.cgi?acc=GSE54388, https://www.ncbi.nlm.nih.gov/geo/query/acc.cgi?acc=gse14407).

Competing interests: The authors declare that the research was conducted in the absence of any commercial or financial relationships that could be construed as a potential conflict of interest.

Funding: National nature science foundation of China (no. 81873111, 81673924, 81774039,82074182)

Authors' contributions: BZ and WD performed the main analysis and drafted the manuscript. BZ and WD designed the research and carried out the introduction and discussion. XC helped to complete the experimental verification, XY helped to finish the image processing. GL and TM assisted in the

preparation of the manuscript. GZ, CD and XW revised the manuscript. All authors wrote, read, and approved the manuscript.

Acknowledgements: Not applicable.

References

1. Webb PM, Jordan SJ. Epidemiology of epithelial ovarian cancer. Best Pract Res Clin Obstet Gynaecol. 2017;41:3–14. doi:10.1016/j.bpobgyn.2016.08.006.
2. Siamakpour-Reihani S, Cobb LP, Jiang C, et al. Differential expression of immune related genes in high-grade ovarian serous carcinoma [published online ahead of print, 2020 Jan 7]. Gynecol Oncol. 2020;S0090-8258(19):31840–2. doi:10.1016/j.ygyno.2019.12.019.
3. Jayson GC, Kohn EC, Kitchener HC, Ledermann JA. Ovarian cancer. Lancet. 2014;384(9951):1376–1388. doi:10.1016/S0140-6736(13)62146-7[3] Grunewald Ledermann T. JA. Targeted Therapies for Ovarian Cancer. Best Pract Res Clin Obstet Gynaecol. 2017;41:139–152. doi:10.1016/j.bpobgyn.2016.12.001.
4. Gorodnova TV, Sokolenko AP, Kuligina E, et al. Principles of clinical management of ovarian cancer. Chin Clin Oncol. 2018;7(6):56. doi:10.21037/cco.2018.10.06.
5. Lee K, Tavassoli FA, Prat J, et al. Tumors of the ovary and peritoneum. In: World Health Organization Classification of Tumors: Pathology and Genetics of Tumors of the Breast and Female Genital Organs. IARC Press; 2003. p. 117.
6. Han LY, Coleman RL. Ovarian cancer staging. Oper Tech Gen Surg. 2007;9(2):53–60.
7. Liu R, Hu R, Zeng Y, et al. Tumour immune cell infiltration and survival after platinum-based chemotherapy in high-grade serous ovarian cancer subtypes: A gene expression-based computational study. EBioMedicine. 2020;51:102602. doi:10.1016/j.ebiom.2019.102602.
8. Chan K. Progress in traditional Chinese medicine. Trends Pharmacol Sci. 1995;16:182–7. doi:10.1016/S0165-6147(00)89019-7.
9. Liu J, Wang S, Zhang Y, Fan HT, Lin HS. Traditional Chinese medicine and cancer: History, present situation, and development. Thorac Cancer. 2015;6:561–9. doi:10.1111/1759-7714.12270.
10. Wang R, Sun Q, Wang F, et al. Efficacy and Safety of Chinese Herbal Medicine on Ovarian Cancer After Reduction Surgery and Adjuvant Chemotherapy: A Systematic Review and Meta-Analysis. Front Oncol. 2019;9:730. doi:10.3389/fonc.2019.00730. Published 2019 Aug 16.
11. Owen S, Ruge F, Gao Y, et al. ShenLingLan Influences the Attachment and Migration of Ovarian Cancer Cells Potentially through the GSK3 Pathway. Medicines (Basel). 2017;4(1):10. doi:10.3390/medicines4010010. Published 2017 Feb 21.
12. Xie Y, Zhang Y, Wei X, et al. Jianpi Huayu Decoction Attenuates the Immunosuppressive Status of H22 Hepatocellular Carcinoma-Bearing Mice: By Targeting Myeloid-Derived Suppressor Cells. Front Pharmacol. 2020 Feb 18;11:16. doi: 10.3389/fphar.2020.00016. PMID: 32140106; PMCID: PMC7042893.

13. Jiang Y, Zhang Y, Luan J, et al. Effects of bufalin on the proliferation of human lung cancer cells and its molecular mechanisms of action. Cytotechnology. 2010;62(6):573–83. doi:10.1007/s10616-010-9310-0.
14. Jiangsu New Medical College. Dictionary of Chinese Medicine. Shanghai, China: Shanghai Printing Factory;1986.5.
15. Li J, Jiang K, Wang LJ, et al. HPLC-MS/MS determination of flavonoids in Gleditsiae Spina for its quality assessment. J Sep Sci. 2018;41(8):1752–63. doi:10.1002/jssc.201701249.
16. Lee SJ, Cho YH, Kim H, et al. Inhibitory effects of the ethanol extract of Gleditsia sinensis thorns on human colon cancer HCT116 cells in vitro and in vivo. Oncol Rep. 2009;22(6):1505–12. doi:10.3892/or_00000594.
17. Jiang Y, Zhong M, Long F, Yang R. Deciphering the Active Ingredients and Molecular Mechanisms of Tripterygium hypoglaucum (Levl.) Hutch against Rheumatoid Arthritis Based on Network Pharmacology. Evid Based Complement Alternat Med. 2020; 2020:2361865. Published 2020 Jan 13. doi:10.1155/2020/2361865.
18. Zhang RZ, Yu SJ, Bai H, Ning K. TCM-Mesh: The database and analytical system for network pharmacology analysis for TCM preparations. Sci Rep. 2017;7(1):2821. doi:10.1038/s41598-017-03039-7. Published 2017 Jun 6.
19. Wang X, Shen Y, Wang S, et al. PharmMapper 2017 update: a web server for potential drug target identification with a comprehensive target pharmacophore database. Nucleic Acids Res. 2017 Jul 3;45(W1):W356-W360. doi: 10.1093/nar/gkx374. PMID: 28472422; PMCID: PMC5793840.
20. Otasek D, Morris JH, Bouças J, Pico AR, Demchak B. Cytoscape Automation: empowering workflow-based network analysis. Genome Biol. 2019 Sep;2(1):185. 20(.
21. Martin A, Ochagavia ME, Rabasa LC, Miranda J, Fernandez-de-Cossio J, Bringas R. BisoGenet: a new tool for gene network building, visualization and analysis. BMC Bioinformatics. 2010;11:91. doi:10.1186/1471-2105-11-91. Published 2010 Feb 17.
22. Tang Yu, Li M, Wang J, et al. CytoNCA: A cytoscape plugin for centrality analysis and evaluation of protein interaction networks[J]. BioSystems,2015,127.
23. Zhou Y, Zhou B, Pache L, et al. Metascape provides a biologist-oriented resource for the analysis of systems-level datasets. Nat Commun. 2019 Apr 3;10(1):1523. doi: 10.1038/s41467-019-09234-6. PMID: 30944313; PMCID: PMC6447622.
24. Hsin KY, Ghosh S, Kitano H. Combining machine learning systems and multiple docking simulation packages to improve docking prediction reliability for network pharmacology. PLoS One. 2013;8(12):e83922. doi:10.1371/journal.pone.0083922. Published 2013 Dec 31.
25. Jiang Y, Liu N, Zhu S, Hu X, Chang D, Liu J. Elucidation of the Mechanisms and Molecular Targets of Yiqi Shexue Formula for Treatment of Primary Immune Thrombocytopenia Based on Network Pharmacology. Front Pharmacol. 2019; 10:1136. Published 2019 Oct 1. doi:10.3389/fphar.2019.01136.

26. Fox E, Oliver T, Rowe M, et al. Indoximod: An Immunometabolic Adjuvant That Empowers T Cell Activity in Cancer. Front Oncol. 2018 Sep 11;8:370. doi: 10.3389/fonc.2018.00370. PMID: 30254983; PMCID: PMC6141803.
27. Tai Z, Lin Y, He Y, et al. Luteolin sensitizes the antiproliferative effect of interferon α/β by activation of Janus kinase/signal transducer and activator of transcription pathway signaling through protein kinase A-mediated inhibition of protein tyrosine phosphatase SHP-2 in cancer cells. Cell Signal. 2014 Mar;26(3):619–28. doi: 10.1016/j.cellsig.2013.11.039. Epub 2013 Dec 12. PMID: 24333668.
28. Ou YC, Li JR, Kuan YH, et al. Luteolin sensitizes human 786-O renal cell carcinoma cells to TRAIL-induced apoptosis. Life Sci. 2014 Apr 1;100(2):110–117. doi: 10.1016/j.lfs.2014.02.002. Epub 2014 Feb 14. PMID: 24530290.
29. Spagnuolo C, Russo GL, Orhan IE, et al. Genistein and cancer: current status, challenges, and future directions. Adv Nutr. 2015 Jul;15(4):408–19. doi:10.3945/an.114.008052. PMID: 26178025; PMCID: PMC4496735. 6) .
30. Kim SH, Jin H, Meng RY, et al. Activating Hippo Pathway via Rassf1 by Ursolic Acid Suppresses the Tumorigenesis of Gastric Cancer. Int J Mol Sci. 2019 Sep 23;20(19):4709. doi: 10.3390/ijms20194709. PMID: 31547587; PMCID: PMC6801984.
31. Albring KF, Weidemüller J, Mittag S, et al. Berberine acts as a natural inhibitor of Wnt/β-catenin signaling–identification of more active 13-arylalkyl derivatives. Biofactors. 2013 Nov-Dec;39(6):652–62. doi:10.1002/biof.1133. Epub 2013 Aug 24. PMID: 23982892.
32. Liu L, Fan J, Ai G, Liu J, Luo N, Li C, Cheng Z. Berberine in combination with cisplatin induces necroptosis and apoptosis in ovarian cancer cells. Biol Res. 2019 Jul 18;52(1):37. doi: 10.1186/s40659-019-0243-6. PMID: 31319879; PMCID: PMC6637630.
33. Barash U, Lapidot M, Zohar Y, et al. Involvement of Heparanase in the Pathogenesis of Mesothelioma: Basic Aspects and Clinical Applications. J Natl Cancer Inst. 2018 Oct 1;110(10):1102–1114. doi: 10.1093/jnci/djy032. PMID: 29579286; PMCID: PMC6186523.
34. Sun X, Zhang G, Nian J, et al. Elevated heparanase expression is associated with poor prognosis in breast cancer: a study based on systematic review and TCGA data. Oncotarget. 2017 Jun 27;8(26):43521–43535. doi: 10.18632/oncotarget.16575. PMID: 28388549; PMCID: PMC5522166.
35. Iozzo RV, Schaefer L. Proteoglycan form and function: A comprehensive nomenclature of proteoglycans. Matrix Biol. 2015 Mar;42:11–55. doi:10.1016/j.matbio.2015.02.003. Epub 2015 Feb 18. PMID: 25701227; PMCID: PMC4859157.
36. Masola V, Bellin G, Gambaro G, Onisto M. Heparanase: A Multitasking Protein Involved in Extracellular Matrix (ECM) Remodeling and Intracellular Events. Cells. 2018 Nov 28;7(12):236. doi: 10.3390/cells7120236. PMID: 30487472; PMCID: PMC6316874.
37. Ellis LM, Staley CA, Liu W, et al. Down-regulation of vascular endothelial growth factor in a human colon carcinoma cell line transfected with an antisense expression vector specific for c-src. J Biol Chem. 1998 Jan 9;273(2):1052-7. doi: 10.1074/jbc.273.2.1052. PMID: 9422768.

38. Ramani VC, Purushothaman A, Stewart MD, Thompson CA, Vlodavsky I, Au JL, Sanderson RD. The heparanase/syndecan-1 axis in cancer: mechanisms and therapies. FEBS J. 2013 May;280(10):2294–306. doi:10.1111/febs.12168. Epub 2013 Mar 4. PMID: 23374281; PMCID: PMC3651779.
39. Zhang GL, Gutter-Kapon L, Ilan N, et al. Significance of host heparanase in promoting tumor growth and metastasis. Matrix Biol. 2020 Nov;93:25–42. doi:10.1016/j.matbio.2020.06.001. Epub 2020 Jun 11. PMID: 32534153; PMCID: PMC7704762.
40. Xu D, McKee CM, Cao Y, Ding Y, Kessler BM, Muschel RJ. Matrix metalloproteinase-9 regulates tumor cell invasion through cleavage of protease nexin-1. Cancer Res. 2010;70(17):6988–98. doi:10.1158/0008-5472.CAN-10-0242.
41. Roy R, Yang J, Moses MA. Matrix metalloproteinases as novel biomarkers and potential therapeutic targets in human cancer. J Clin Oncol. 2009;27(31):5287–97. doi:10.1200/JCO.2009.23.5556.
42. Van Roy F, Berx G. The cell-cell adhesion molecule E-cadherin. Cell Mol Life Sci. 2008 Nov;65(23):3756-88. doi: 10.1007/s00018-008-8281-1. PMID: 18726070.
43. Katoh M. Multi–layered prevention and treatment of chronic inflammation, organ fibrosis and cancer associated with canonical WNT/β–catenin signaling activation (Review). Int J Mol Med. 2018 Aug;42(2):713–25. doi:10.3892/ijmm.2018.3689. Epub 2018 May 17. PMID: 29786110; PMCID: PMC6034925.
44. Morin PJ, Sparks AB, Korinek V, et al. Activation of beta-catenin-Tcf signaling in colon cancer by mutations in beta-catenin or APC. Science. 1997 Mar 21;275(5307):1787-90. doi: 10.1126/science.275.5307.1787. PMID: 9065402.
45. Xia P, Xu XY. PI3K/Akt/mTOR signaling pathway in cancer stem cells: from basic research to clinical application. Am J Cancer Res. 2015 Apr 15;5(5):1602-9. PMID: 26175931; PMCID: PMC4497429.
46. Karar J, Maity A. PI3K/AKT/mTOR Pathway in Angiogenesis. Front Mol Neurosci. 2011;4:51. doi:10.3389/fnmol.2011.00051. Published 2011 Dec 2.
47. Cancer Genome Atlas Research Network. Integrated genomic analyses of ovarian carcinoma [published correction appears in Nature. 2012 Oct 11;490(7419):298]. Nature. 2011;474(7353):609–615. Published 2011 Jun 29. doi:10.1038/nature10166.
48. Hildebrand PW, Rose AS, Tiemann JKS. Bringing Molecular Dynamics Simulation Data into View. Trends Biochem Sci. 2019 Nov;44(11):902–13. doi:10.1016/j.tibs.2019.06.004. Epub 2019 Jul 10. PMID: 31301982.

Tables

Due to technical limitations, Table 1 is only available as a download in the Supplemental Files section.

Table 2: Candidate active components in Gleditsiae Spina

ID	MOL NAME
GS1	D-(+)-Glucose
GS2	Pantothenic acid
GS3	Salicylic acid
GS4	Adipic acid
GS5	Vanillic acid
GS6	Vanillin
GS7	Ferulic acid
GS8	Phloroglucinol
GS9	D-(+)-Tryptophan
GS10	trans-Cinnamic acid
GS11	Fustin
GS12	Hydrocinnamic acid
GS13	Tyramine
GS14	Robinetin
GS15	Luteolin
GS16	Azelaic acid
GS17	Genistein
GS18	Hexadecanedioic acid
GS19	Ursolic acid
GS20	Oleanolic acid
GS21	Methyl cinnamate
GS22	Citral
GS23	Berberine
GS24	Rhamnetin
GS25	Stigmastane-3,6-dione
GS26	Catechin

Figures

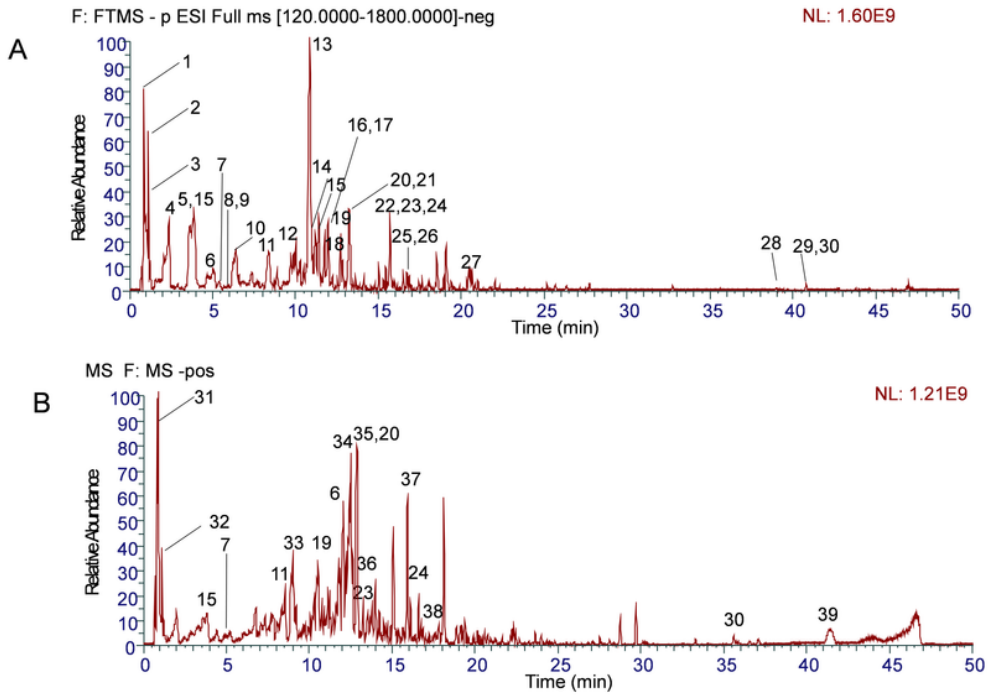

Figure 1

UHPLC-Q-Exactive Orbitrap MS identification results of the main chemical components in the extract of Gleditsiae Spina. A total ion current graph in positive ion and negative ion mode; B total ion current graph in negative ion and negative ion mode.

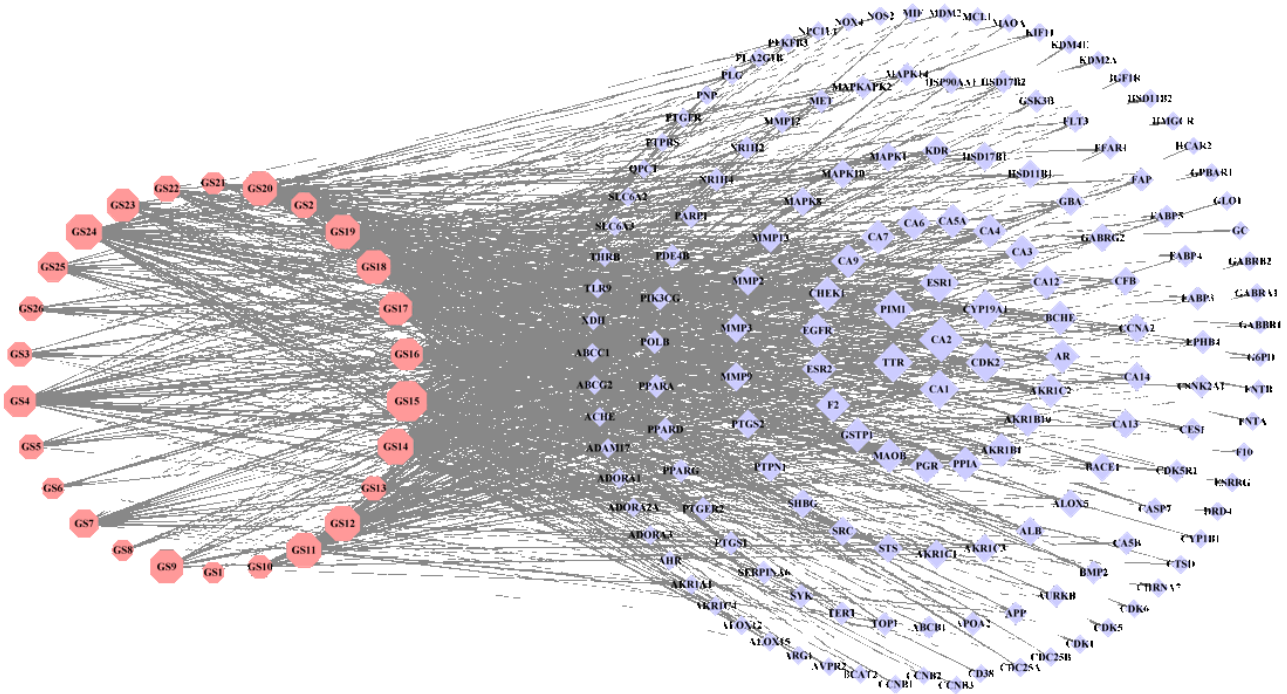

Figure 2

Active component-target network map of Gleditsiae Spina. The purple labels represent the targets of the action of active components in the figure; the red labels represent 26 Gleditsiae Spina active components.

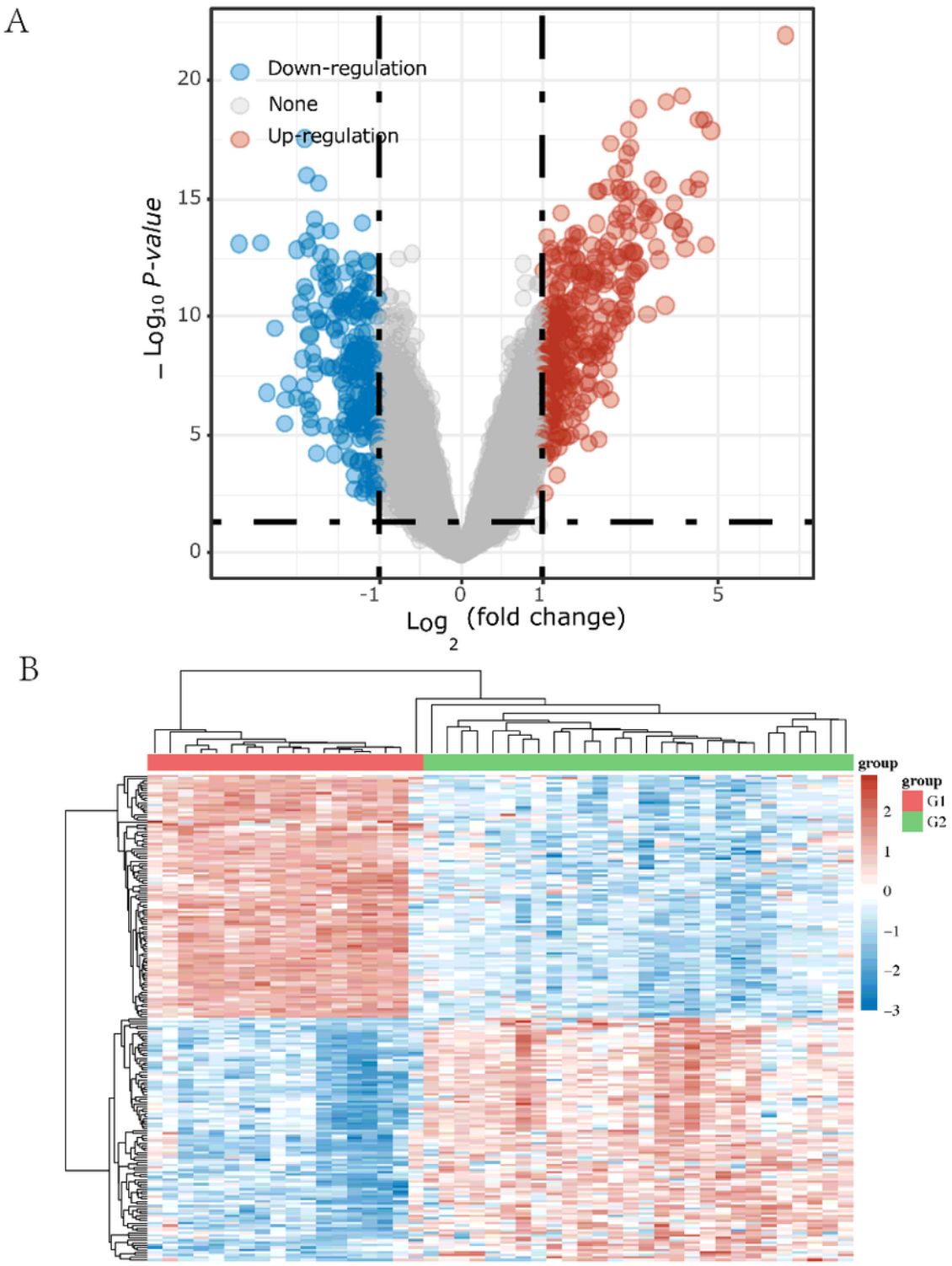

Figure 3

Volcano plot of differentially expressed genes. The abscissa represents the fold change in gene expression, and the ordinate represents the statistical significance of the change in gene expression. Red dots represent genes with significantly increased expression and blue dots represent genes with reduced

expression (A). Heatmap of differentially expressed genes. Heat map shows differentially expressed genes in normal ovarian tissue (G1) and HGSC (G2). Up-regulated and down-regulated genes are shown (B).

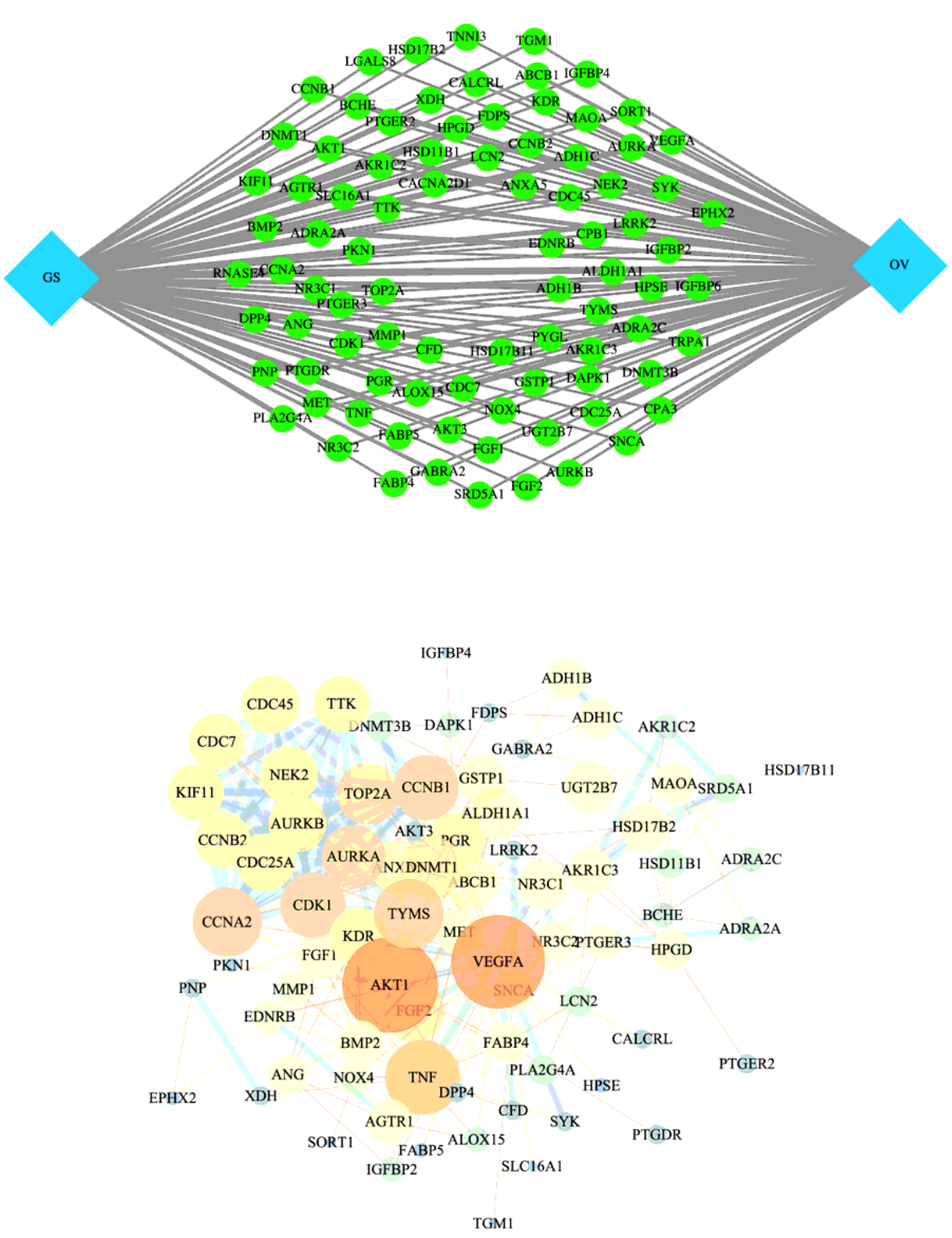

Figure 4

The key targets of the Gleditsiae Spina treating for Ovarian Cancer(A) and the PPI network(B).

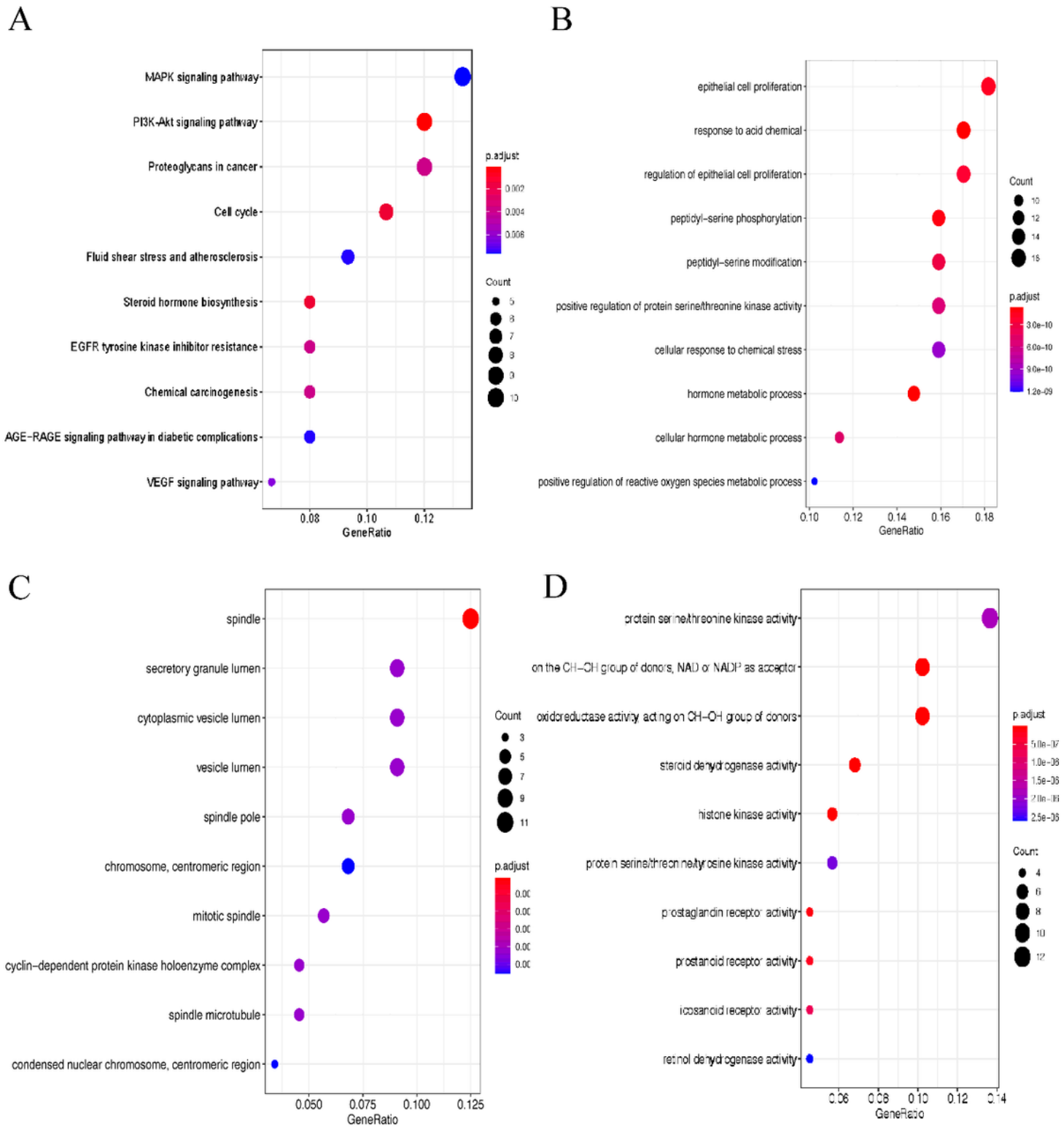

Figure 5

Bubble diagram of GO and KEGG enrichment of key targets for Gleditsiae Spina for treatment of HGSC. A: KEGG analyse; B: GO BP analyse; C: GO CC analyse; D: GO MF analyse. Pathways that had significant changes of log10(P)<0.05 were identified. Size of the spot represents number of genes and color represents log10(P) value.

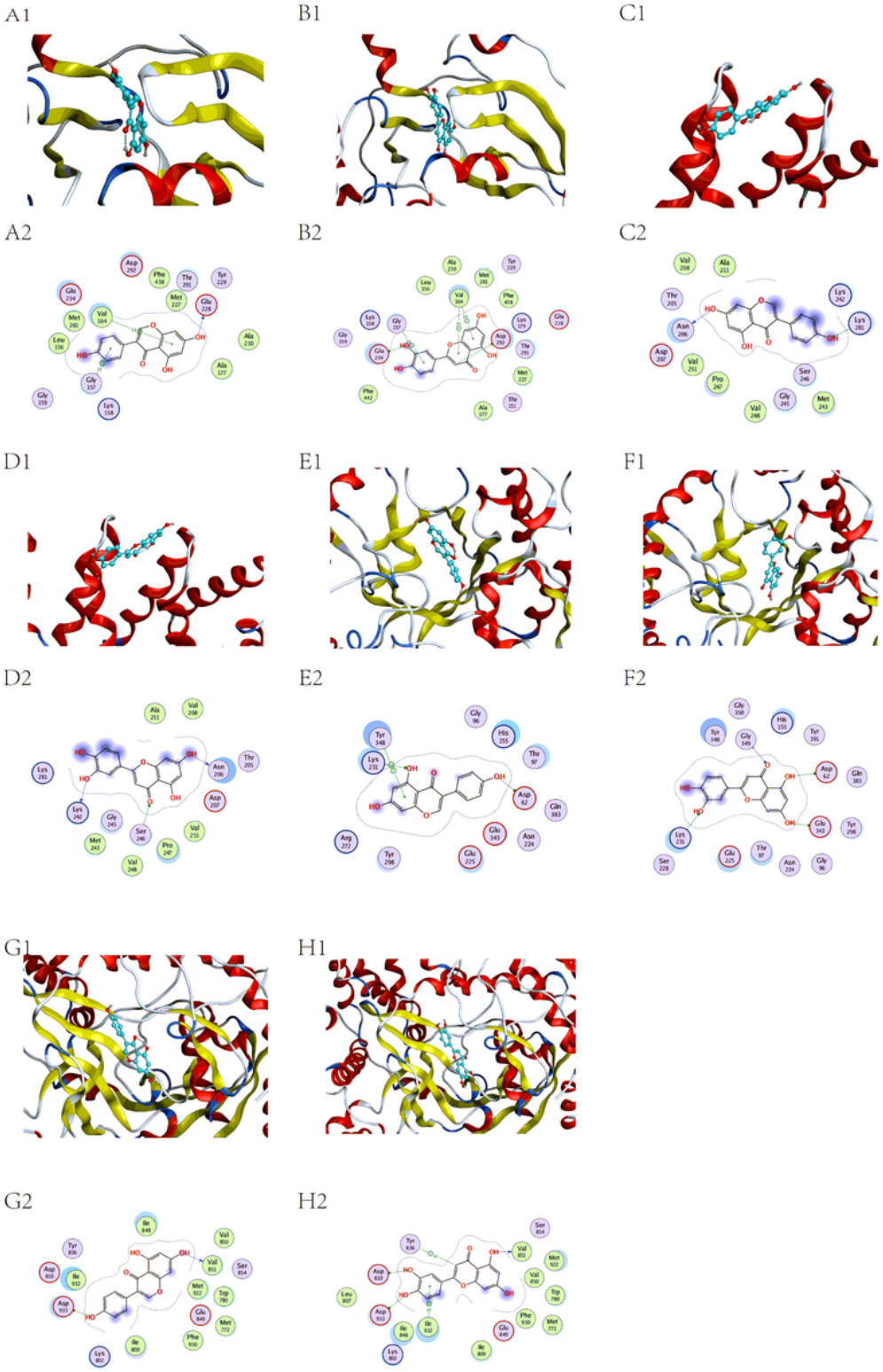

Figure 6

Molecular docking of compounds with core targets: A: AKT1-Genistein; B: AKT1-Luteolin; C: CTNNB1-Genistein; D: CTNNB1-Luteolin; E: HPSE-Genistein; F: HPSE-Luteolin; G: PIK3CA-Genistein; H: PIK3CA-Luteolin.

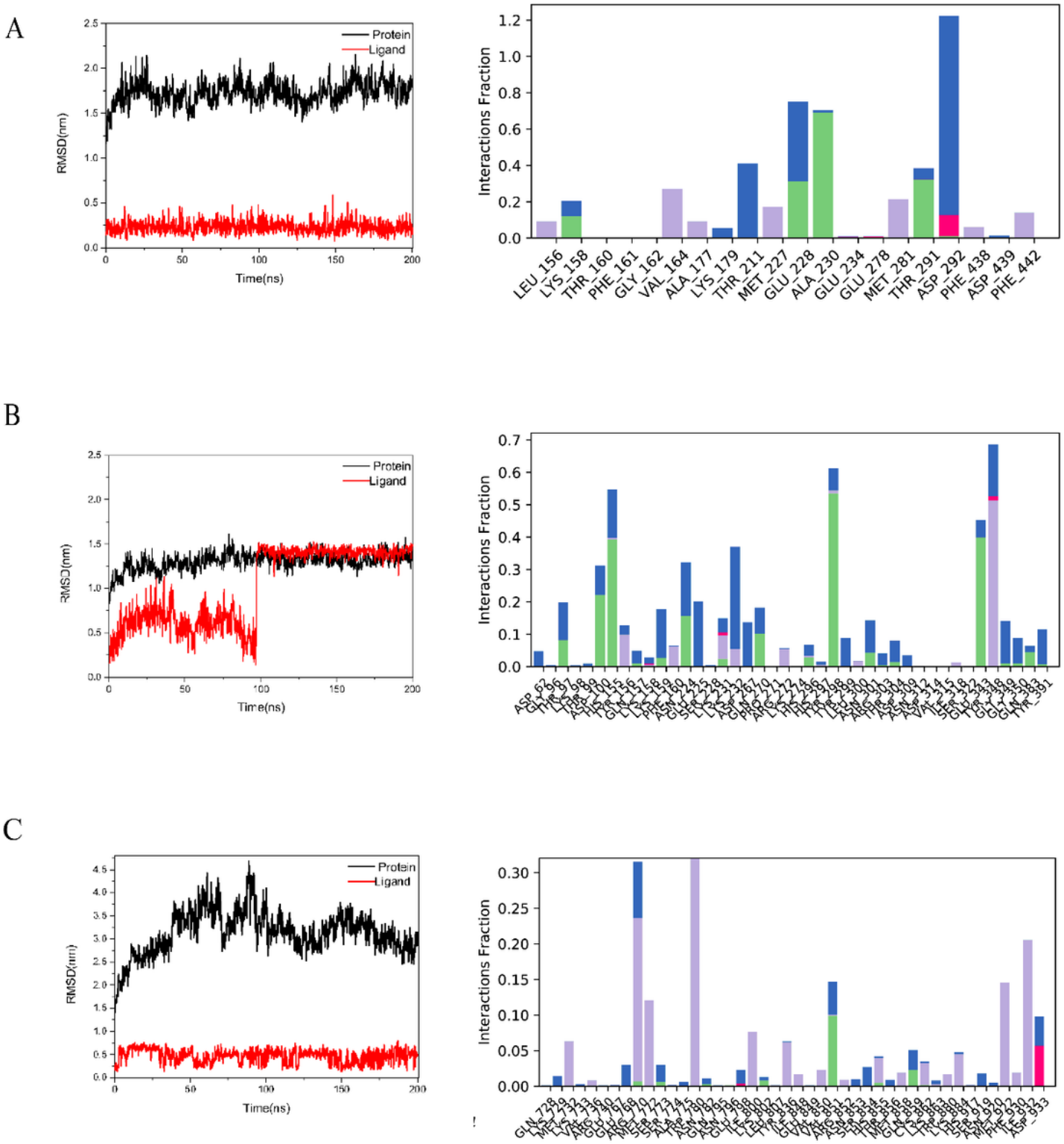

Figure 7

Molecular dynamics simulation of compounds with core targets: RMSD plot during molecular dynamics simulations of AKT1 with Genistein (A), HPSE with Luteolin (B); PI3K with Berberine (C).

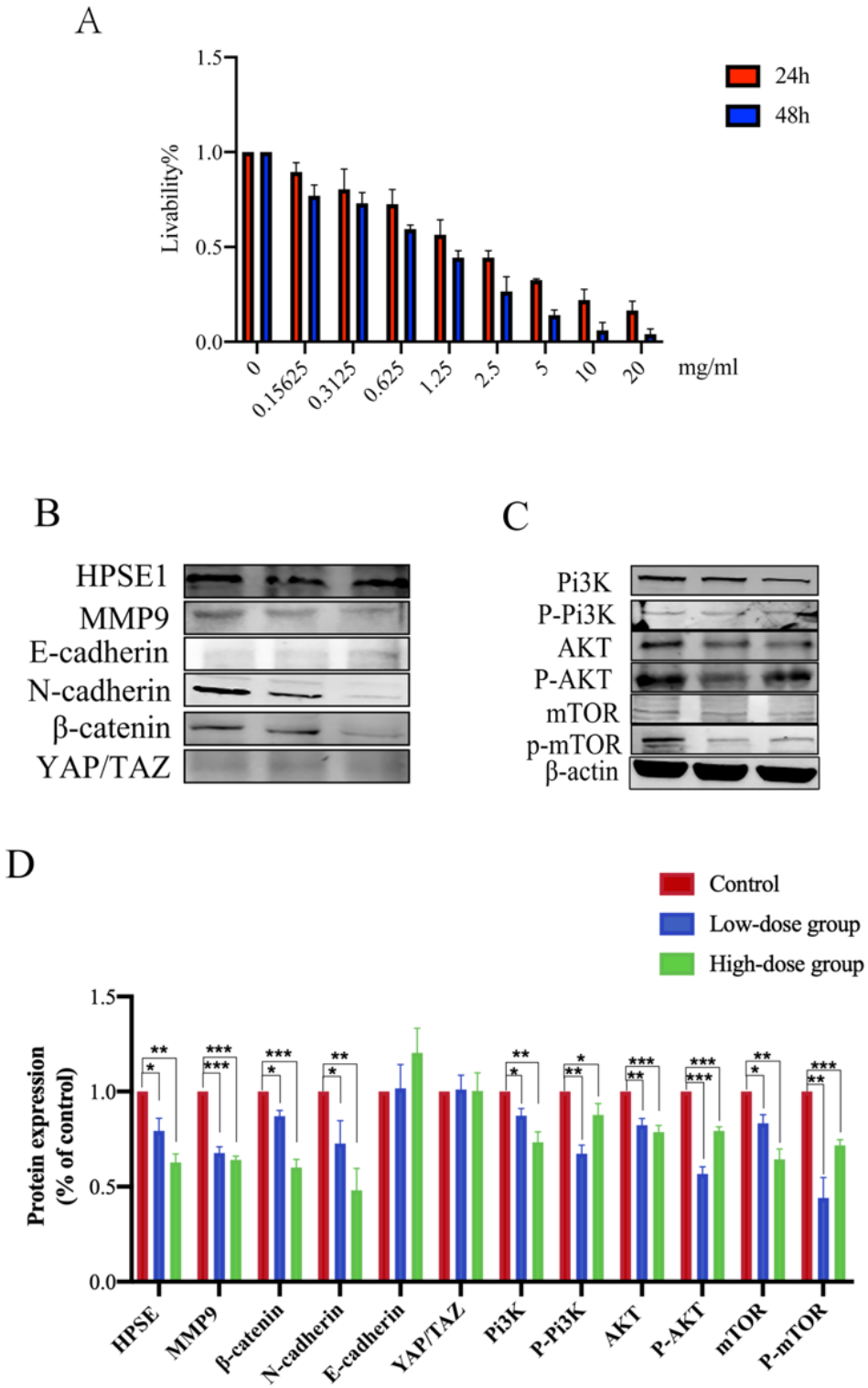

Figure 8

The cellular verification results. A: Dose-dependent inhibitory effect of Gleditsiae Spina on ovarian cancer cell proliferation. B and C: After exposure to the Gleditsiae Spina for 24 h, the total protein from each cell lysate was analyzed by Western blotting to measure the expression of proteins. D: Data are presented as the mean ± SD and normalized to β-actin (* $P < 0.05$, ** $P < 0.01$, *** $P < 0.001$).

Supplementary Files

This is a list of supplementary files associated with this preprint. Click to download.

- Table1.docx